FAULT RUPTURE AND KINEMATIC DISTRESS OF EARTH FILLED EMBANKMENTS

V. Zania[1], Y. Tsompanakis[2] and P.N. Psarropoulos[3]

[1] *Doctoral Candidate, Dept. of Applied Mechanics, Technical University of Crete, Chania, Greece*
[2] *Asst. Professor, Dept. of Applied Mechanics, Technical University of Crete, Chania, Greece*
[3] *Post-Doctoral Researcher, Dept. of Applied Mechanics, Technical University of Crete, Chania, Greece*
Email: zaniab@tee.gr, jt@science.tuc.gr, & prod@central.ntua.gr

ABSTRACT :

According to common practice the seismic design of any type of structure or infrastructure is focused on the inertial loading and the resulting distress generated due to the imposed ground shaking. Regarding the effects of fault rupture on seismic design, seismic norms contain mainly provisions that are related to the citation of the structures/geostructures. Moreover, the additional distress imposed to large-scale structures (like bridges, lifelines, dams, or earth-filled embankments) by the applied permanent deformations produced during a potential fault rupture may not be possible to be avoided. As in many cases the exact location of faults is not known, especially when surface scarps are not present, the consequences of the permanent deformations in large-scale structures should be carefully and realistically evaluated. The current study examines numerically the behavior of earth-filled embankments, focusing on their kinematic distress due to fault rupture propagation. Apart from a brief literature review of the problem, a parametric study is conducted in order to investigate the role of the main parameters involved. The results indicate that the effects of fault rupturing in earth-filled embankments should be treated with caution. Additionally, the resulting kinematic distress should not be disregarded in the stability assessment, and therefore, it should be taken into account in the overall seismic design of the embankments.

KEYWORDS: embankments, active faults, rupture, permanent deformations, kinematic distress.

1. INTRODUCTION

Seismic distress of structures may arise as a result of any of the two types of earthquake loading. The first component of seismic distress is related to the strong ground motion provided by the waves propagating from the seismic source, while the second one is related to earthquake induced permanent ground deformation. In the current study the behavior of earth-filled embankments subjected to permanent ground deformation, and more specifically to fault rupture, is investigated. Earth -lled embankments (either as a part of a transportation system, or in the case of a dam) are geostructures, a potential damage of which entails undesirable socio-economical consequences. Additionally, the effect of a fault dislocation on the stability of the slopes of a soil embankment has not been yet fully resolved.

Concerning the fault rupture propagation through soft soil deposits, intense research interest has been observed in the literature. The mechanism of the fault rupture propagation has been shown to be affected by the fault type, the magnitude of fault displacement, the fault dip angle, and the mechanical properties of the soil material overlying the fault tip. More specifically, studies based on field observations report that strike-slip faults propagate almost vertically producing a relatively narrow zone of deformation (Bray et al., 1994a). Furthermore, the angle of fault rupture propagation reduces near the ground surface in the case of reverse faults, while the opposite holds for normal faults resulting to even vertical surface exposure (Lade et al., 1984). Normal faults are also characterized by a secondary failure surface, which is commonly developed in the case of a small dip angle, and emerges as a graben. These observations are consistent with the results of small-scale sandbox experiments conducted by Cole and Lade (1984). Moreover, Cole and Lade have shown that the relative amount of fault dislocation (relatively to the height of the soil layer) required for a reverse fault to reach the ground surface is larger than the corresponding of a normal fault. Duncan and Lefebvre (1983) examined

also the normal and reverse fault propagation via finite element analyses and derived similar to the aforementioned results, concluding to a parallelization of reverse and normal fault propagation mechanism with the passive and active soil resistance.

Recently numerical methods have been also utilized for the investigation of the deformations developed by fault propagation through soil layers. The finite element method (Bray et al. 1994b, Lin et al. 2006 and Anastasopoulos et al., 2007) and the finite difference method (Papadimitriou et al., 2007) have been employed, and valuable aspects of the problem have been addressed. Additionally, the aforementioned studies have shown that proper implementation of numerical methods requires: (a) a realistic modeling of soil nonlinear behavior through an appropriate constitutive model, (b) dense (finite element or finite difference) mesh, and (c) sufficient model size in order to avoid any arising boundary effects. In contrast, earlier studies provided unrealistic results (Scott and Schoustra, 1974) probably due to the inadequate application of the modified von Mises criterion for modeling of soil material non-linearity. Bray et al. (1994b), after verifying their numerical methodology by small scale experiments, have shown that reverse fault propagation through clayey soil is related to bending of the upthrown block over the downthrown. According to Lin et al. (2006) the most important parameters affecting the propagation of a reverse fault through sandy soil are the Young's modulus and the dilation angle. Also, in accordance to the observations of Cole and Lade (1984), Anastasopoulos et al. (2007) have concluded that the magnitude of fault dislocation for the rupture to reach surface increases in case of loose sand compared to dense sand, and in case of reverse fault compared to normal fault. Moreover, Papadimitriou et al. (2007) have shown that in clayey soils the magnitude of fault dislocation for the rupture to reach surface is lower than the corresponding of sandy soils.

The current study investigates the fault rupture propagation through an earth embankment. Therefore, finite element analyses were conducted aiming to evaluate the stability of the geostructure for both cases of normal and reverse fault propagation, which were considered as the most critical. The adopted numerical methodology was qualitatively verified through field observations and through published numerical results. One of the main aspects of the problem that was examined is the effect of the slopes of the embankment on the fault propagation. Two possible locations of the fault tip along the foundation of the embankment were examined for three cases of angle of fault rupture. The developed surface deformation was determined, and important issues of the examined phenomena were highlighted.

2. DESCRIPTION OF NUMERICAL ANALYSIS

The finite element modeling was conducted using ABAQUS (2004) software. Initially, a one-dimensional model was analyzed to verify the adopted procedure. Figure 1 shows the finite element mesh, which was discretized with plane strain quadrilateral elements. The mesh was on purpose finer in the region of the fault tip and coarser close to the boundaries, since a relatively large mesh was required in order to avoid boundary effects. The horizontal length of the mesh was four times the height (20m), which was also considered sufficient in other numerical studies (Bray et al., 1994b, Anastasopoulos et al,. 2007, Papadimitriou et al., 2007). Initially, the cases of a normal and a reverse fault of 45^o dip angle propagating through a dense sandy soil layer with angle of friction equal to 50^o and angle of dilation 20^o were investigated. The soil material non-linearity was modeled using the Mohr-Coulomb failure criterion, extended to incorporate the material's strain softening behavior by utilizing a user-defined subroutine. The fault displacement was considered for both cases to be equal to 1m.

In Figure 2 the plastic strain distribution on the case of the normal fault is shown. The concentration of the contours allows the estimation of the developed failure surfaces due to the fault movement. Concurrently, the failure mode reported by Bray et al (1994a) for normal faults of small dip angle propagating through stiff soils is presented. It is obvious that both primary and secondary failure surfaces are developed, and the failure pattern is comparable to the field observations, since a graben is also observed. Moreover, the normalized displacement required for the fault to reach the ground surface (δ/H) is equal to 1%, which is comparable to the

corresponding value reported by Cole and Lade (1984). Additionally, the computed surface deformation is qualitatively in good agreement with the reported results of other numerical studies referring to normal fault propagation through dense sand (Anastasopoulos et al., 2007 and Papadimitriou et al., 2007).

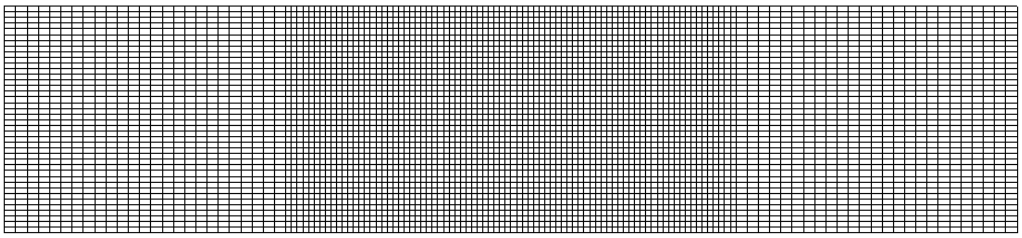

Figure 1 Finite element mesh for the verification of the numerical procedure

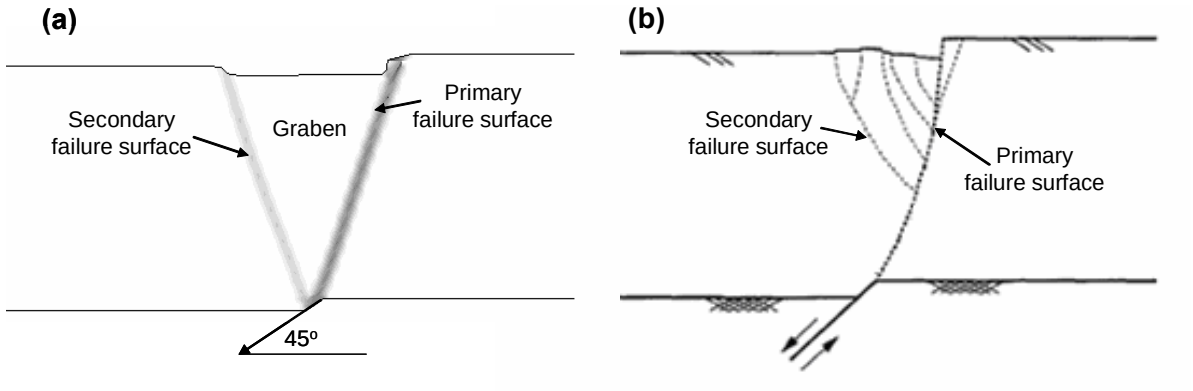

Figure 2 Failure surfaces developed during the propagation of a normal fault through dense sand obtained by: (a) the current numerical study, and (b) field observations by Bray et al. (1994a).

The analysis of the propagation of a reverse fault through a dense sandy soil layer has provided the plastic strain variation shown in Figure 3a. The developed failure surface compares well with the corresponding surface reported by Bray et al. (1994a) and bending of the upthrown block over the downthrown is also observed. Additionally, the normalized displacement required for the fault to reach the ground surface (δ/H) is equal to 3%, which is comparable to the corresponding reported by Cole and Lade (1984). The surface deformation in published numerical studies referring to reverse fault propagation through dense sand (Anastasopoulos et al., 2007, Papadimitriou et al., 2007) is quite similar to the surface deformation calculated in the current study. Concluding, for both examined fault types the adopted numerical procedure provided satisfactory results compared to other studies in the literature, based either on field observations or in numerical simulations.

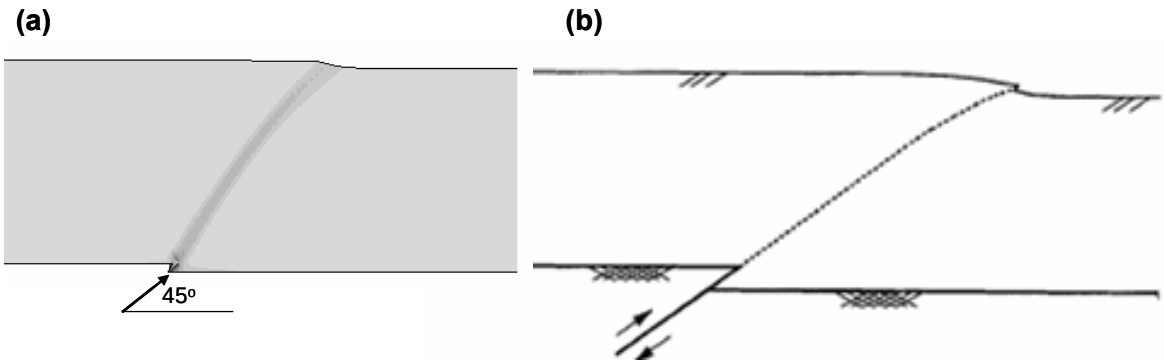

Figure 3 Failure surfaces developed during the propagation of a reverse fault through dense sand obtained by:

(a) the current numerical study, and (b) field observations by Bray et al. (1994a).

3. TWO-DIMENSIONAL NUMERICAL ANALYSES

The one-dimensional soil layer is generally an assumption, considered rather accurate for cases characterized by distant side boundaries. Earth embankments are geostructures with a deck of finite length, and therefore the effect of side boundaries on fault propagation should be evaluated. For this purpose, the embankment shown in Figure 4 is analyzed. Its height is equal to 20m and it is characterized by smooth slope inclination 1:3 (V: H). In addition, as already mentioned, the propagation of the fault rupture is investigated for two different positions of the fault tip, which are also shown in Figure 4. The first position selected (point A) is considered at the axis of symmetry of the structure, while the second one (point B) lies at a distance equal to 20m from the crest of the embankment. The finite element mesh developed for each case was different in order to achieve higher accuracy. A denser discretization of quadrilateral plane strain elements was used at the region of the fault tip.

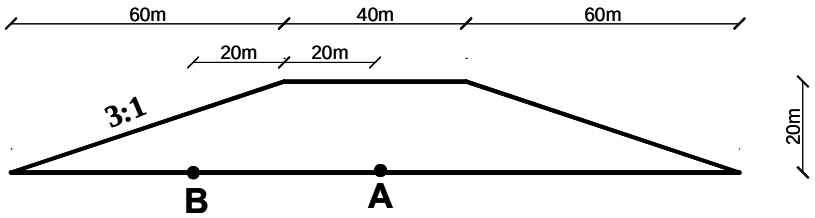

Figure 4 Cross-section of the examined embankment. The two examined positions of the fault tip (A and B) are also shown.

Initially, the case analyzed is the propagation of a normal and a reverse fault with dip angle equal to 45° and fault tip at point A. In order to estimate the effect of the side boundaries, both results of one- and two-dimensional analyses are presented. Figure 5a shows the variation of normalized (relatively to the height of the embankment) vertical displacement as a function of the deformed horizontal coordinate. It is obvious that, although the geometric characteristics of the embankment imply that the surface exposure of the fault is expected at the crest of the embankment (x/H=1), the fault rupture propagates with an increased angle and therefore reaches the surface at a distance of 0.85H from point A. This observation is probably related also to the fact that results of one-dimensional analyses (continuous line) are almost identical to the corresponding ones of the two-dimensional analyses (symbols). The variation of the surface deformations indicate also that the region of significant deformations is between 0.85H and 0.5H, while the graben is formed at relative displacement (δ/H) equal to 2%. In the case of the reverse fault (Figure 5b) the deformation pattern of the surface is similar in the one-dimensional and two-dimensional analyses only for minor relative displacement (δ/H=1%). The increase of the fault dislocation (δ/H = 2% and 3%) results to underestimation of the normalized vertical displacement by the one-dimensional modeling for a distance equal to 0.25H from the crest of the embankment.

Subsequently, the cases of a normal and a reverse fault with dip angle equal to 60° and a fault with angle equal to 90° were analyzed at the same positions A and B. The results of the aforementioned cases are depicted in Figures 6 and 7. It is obvious that a secondary failure surface, and therefore a graben, is not formed as an outcome of the normal fault propagation possibly due to the higher dip angle of the fault. Additionally, the surface exposure of the fault is observed at a distance almost equal to 0.5H, where the direct projection of the fault plane would be expected. The zone of surface deformation is relatively narrow extending from 0.5H to 0.75H. On the other hand, the fault of dip angle equal to 90° propagates almost vertically, thus, the surface deformations are concentrated at the axis of symmetry of the embankment for all the computed levels of relative displacement. The width of the developed zone of deformation during the propagation of the reverse fault increases as the fault dislocation increases. Initially, for small magnitude of fault displacement (δ/H=1%) the surface exposure of the fault is located at a distance equal to 0.25H from the fault tip, indicating an angle of fault rupture propagation equal to 75°. The increase of the fault displacement to δ/H=4% is related to a zone of surface deformation extending from 0.25H to the crest of the embankment, indicating the decrease of the angle

of the fault rupture propagation.

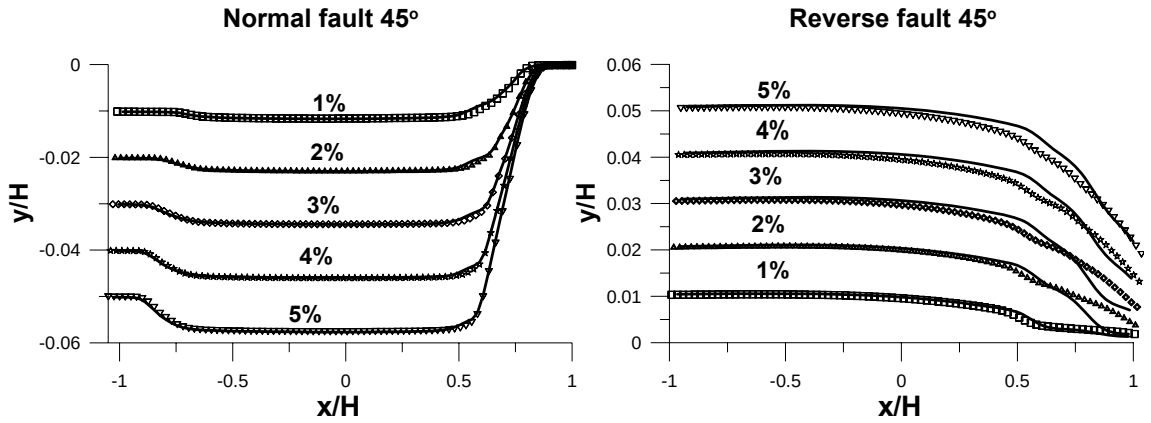

Figure 5 Fault tip at point A: Variation of the normalized to the height of the embankment vertical displacement of the surface relatively to the normalized to the height of the embankment deformed horizontal coordinate. Results are presented for five levels of relative displacement (δ/R): 1%, 2%, 3%, 4% and 5%.

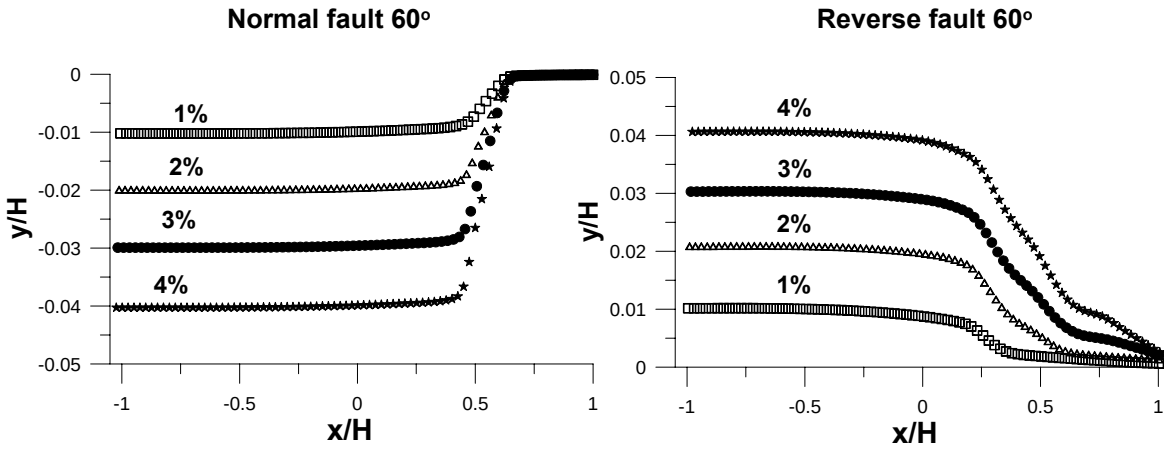

Figure 6 Fault tip at point A: Variation of the normalized to the height of the embankment vertical displacement of the surface relatively to the normalized to the height of the embankment deformed horizontal coordinate. Results are presented for four levels of relative displacement (δ/R): 1%, 2%, 3%, and 4%.

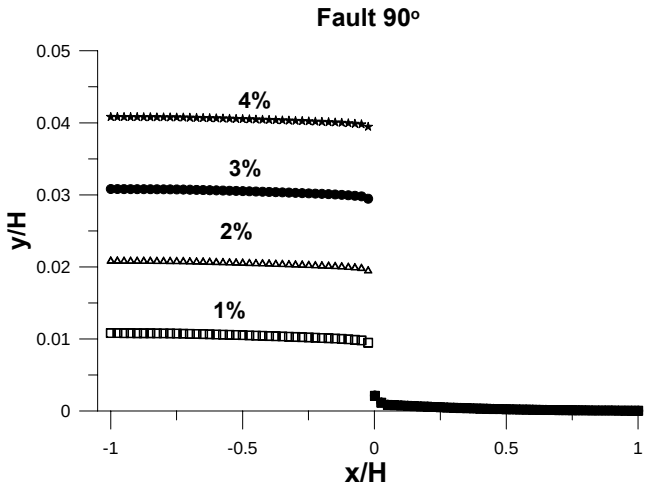

Figure 7 Fault tip at point A: Variation of the normalized to the height of the embankment vertical displacement of the surface relatively to the normalized to the height of the embankment deformed horizontal coordinate.

Results are presented for four levels of relative displacement (δ/R): 1%, 2%, 3%, and 4%. Furthermore, the case of the fault tip located under the slopes of the embankment is investigated. For this purpose the propagation of a normal fault with dip angle equal to 45° and 60° and fault tip located at point B are analyzed. Results of the aforementioned cases are presented in Figure 8 in terms of horizontal and vertical displacement with respect to the horizontal component of the distance from the fault tip (x=0m). Note that due to the geometry of the embankment the fault crest is located at x=20m. In the same figure the corresponding results of the analyses for location of the fault tip at point A are also shown (symbols). For the case of dip angle equal to 45° the angle of fault propagation as well as the magnitude of displacement required for surface exposure of the fault are quite similar for the two positions of the fault tip. Nevertheless, the distance at which the secondary failure surface is observed is not comparable for the two examined positions, possibly due to the inclined surface of the slopes of the embankment. Additionally, in both examined cases the width of the zone of deformations and the magnitude of plastic deformations are increased when the fault tip is located under the slope of the embankment (point B).

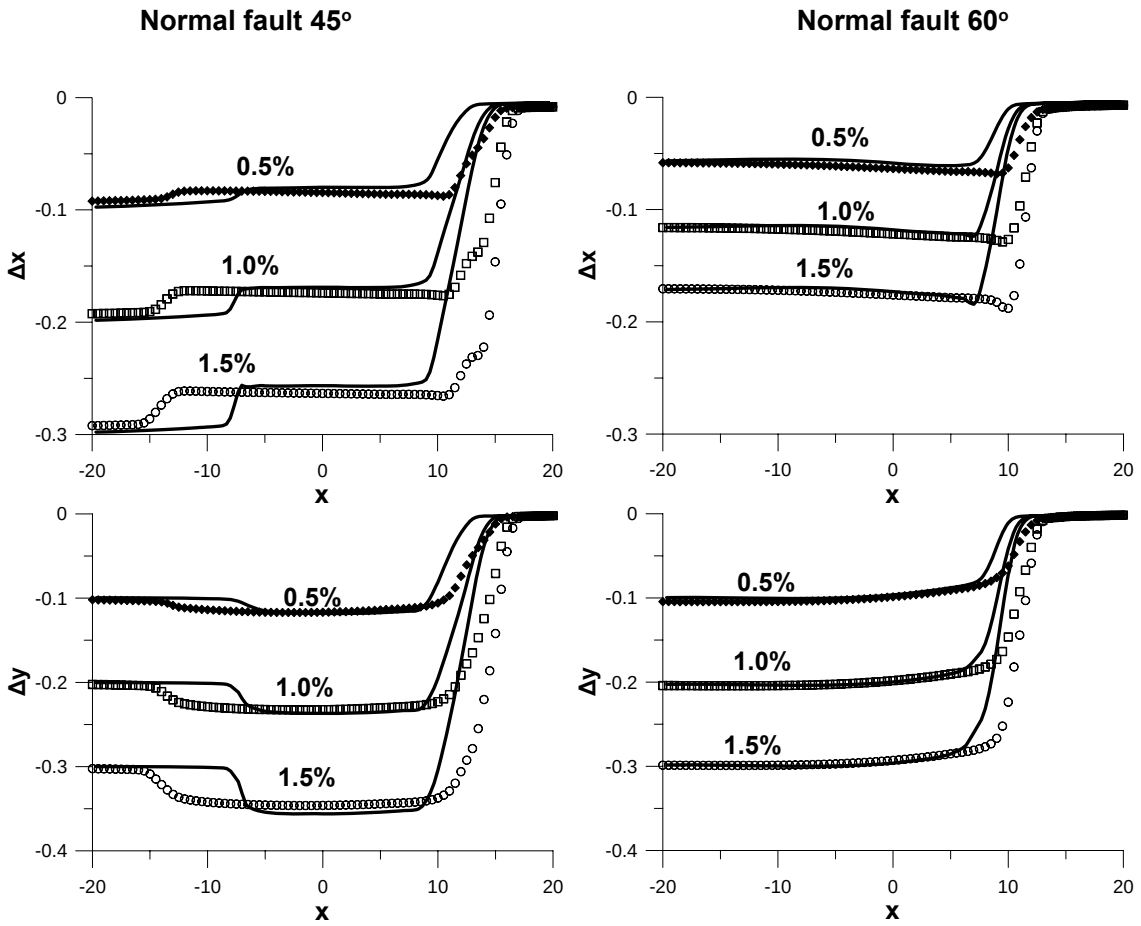

Figure 8 Fault tip at point B: Variation of the horizontal and vertical displacement of the surface relatively to the horizontal component of the distance from the fault tip. Results are presented for dip angle equal to: (a) 45° and (b) 60°. The symbols represent the corresponding results for fault tip at point A.

4. CONCLUSIONS

In the current study the mechanism of the fault rupture propagation through a soil embankment was investigated. In the first part of the numerical investigation the adopted numerical procedure was quantitatively verified by reported field observations, experimental results and results of other published numerical simulations. The results of this study indicate that the two-dimensional geometry of a geostructure may affect

substantially the pattern and the magnitude of the developed deformations with respect to: (a) the position of the fault tip, (b) the dip angle of the fault, and (c) the fault type. More specifically, surface deformations in the region of the crest are increased in the case of a reverse fault, even if the fault tip is located in a sufficient distance and the dip angle is large. This implies that, reverse fault propagation may produce instability at the crest of the embankment. Additionally, surface deformations are increased when the fault tip is located under the slopes of the embankment. These observations indicate that the seismic design of embankments should take into account the potential distress from a fault displacement.

ACKNOWLEDGMENTS

This paper is part of the 03ED454 research project, implemented within the framework of the "Reinforcement Programme of Human Research Manpower" (PENED) and co-financed by National and Community funds (75% from E.U.- European Social Fund and 25% from the Greek Ministry of Development- General Secretariat of Research and Technology).

REFERENCES

ABAQUS (2004). "Analysis User's Manual Version 6.4", ABAQUS Inc, USA.

Anastasopoulos, I., Gazetas, G., Bransby, M.F., Davies, M.C.R., and El Nahas, A. (2007). Fault rupture propagation through sand: Finite–element analysis and validation through centrifuge experiments. *Journal of Geotechnical and Geoenvironmental Engineering*, **133: 8**, 943-958.

Bray, J.D., Seed, R.B., Cluff, L.S., and Seed, H.B. (1994a). Earthquake fault rupture propagation through soil. *Journal of Geotechnical Engineering*, **120: 3**, 543-561.

Bray, J.D., Seed, R.B., and Seed, H.B. (1994b). Analysis of earthquake fault rupture propagation through cohesive soil. *Journal of Geotechnical Engineering*, **120: 3**, 562-580.

Cole, D.A., and Lade, P.V. (1984). Influence zones in alluvium over dip-slip faults. *Journal of Geotechnical Engineering*, **110: 5**, 599-615.

Duncan, J.M., and Lefebvre, G. (1973). Earth pressures on structures due to fault movement. *Journal of the Soil Mechanics and Foundations Division*, **99: SM12**, 1153-1163.

Lade, P.V., Cole, D.A., and Cummings, D. (1984). Multiple failure surfaces over dip-slip faults. *Journal of Geotechnical Engineering*, **110: 5**, 616-627.

Lin, M.-L., Chung, C.-F., and Jeng, F.-S. (2006). Deformation of overburden soil induced by thrust fault slip. *Engineering Geology*, **88**, 70-89.

Papadimitriou, A., Loukidis, D., Bouckovalas, G., and Karamitros, D. (2007). Zone of excessive ground surface distortion due to dip-slip fault rupture. Proc. of the 4th International Conference on Earthquake Geotechnical Engineering, June 25-28, Thessaloniki, Greece.

Scott, R.F. and Schoustra, J.J. (1974). Nuclear power plant siting on deep alluvium. *Journal of Geotechnical Engineering Division*, **100:4**, 449-459.